Multinuclear Variable-temperature Nuclear Magnetic Resonance Study of Rhodium Carbonyl Clusters containing Encapsulated Heteroatoms: Ligand and Metal Polyhedral Rearrangements

Brian T. Heaton,* Luisella Strona, and Roberto Della Pergola
Chemical Laboratory, University of Kent, Canterbury CT2 7NH
José L. Vidal * and Richard C. Schoening
Union Carbide Corporation, Research and Development Department, P.O. Box 8361, South Charleston, West Virginia 25304, U.S.A.

Variable-temperature multinuclear n.m.r. studies (^{13}C, ^{13}C-{^{103}Rh}, ^{13}C-{^{31}P}, and ^{31}P) are reported for $[Rh_9E(CO)_{21}]^{2-}$, $[Rh_{10}E(CO)_{22}]^{3-}$ (E = P or As), and $[Rh_{12}Sb(CO)_{27}]^{3-}$. In all cases, complete fluxionality of both the carbonyl and metal polyhedra are observed at high temperatures, and at low temperatures it has been possible to obtain spectra for the Rh_9 and Rh_{10} clusters, which are fully consistent with their solid-state structures, thus allowing a complete spectroscopic assignment; the Rh_{12} cluster is still fluxional in solution at $-97\ °C$.

A variety of high nuclearity carbonyl clusters containing interstitial heteroatoms is now known. The recent discovery of the closely related clusters $[Rh_9E(CO)_{21}]^{2-}$ and $[Rh_{10}E(CO)_{22}]^{3-}$ (E = P or As)[1-3] enabled us to carry out variable-temperature n.m.r. measurements in order to compare their behaviour in solution and spectroscopic data. These clusters are particularly interesting since previous ^{103}Rh n.m.r. measurements on $[Rh_9P(CO)_{21}]^{2-}$ showed that the metal skeleton is fluxional.[4] We also report related studies on $[Rh_{12}Sb(CO)_{27}]^{3-}$.[5]

Experimental

The syntheses of the anionic carbonyl clusters $[Rh_9E(CO)_{21}]^{2-}$, $[Rh_{10}E(CO)_{22}]^{3-}$ (E = P or As), and $[Rh_{12}Sb(CO)_{27}]^{3-}$ were conducted following previously described procedures.[1-3,5,6] All manipulations were carried out using Schlenk-tube techniques under an argon atmosphere and solvents were dried using conventional procedures and stored under argon.

The solutions for n.m.r. measurements were prepared by saturating perdeuterioacetone (3 cm³) with either the $[NEt_3(CH_2Ph)]^+$ or $[Cs\{Me(OCH_2CH_2)_4OMe\}]^+$ salts of the cluster anions (0.4—0.6 g). The complexes were enriched by direct exchange of solutions with ^{13}CO under ambient conditions using standard vacuum-line techniques; the final enrichment was *ca.* 40%. The ^{13}C-enriched samples were transferred *via* syringe into an evacuated n.m.r. tube placed inside a Schlenk container under argon; the tubes were then sealed.

Carbon-13 n.m.r. spectra were recorded on either a Varian XL-100 n.m.r. spectrometer, equipped with Fourier-transform capabilities, using 12-mm sample tubes, or on a JEOL PS-100 or Bruker WH360 Fourier-transform spectrometer as described previously;[7] ^{13}C-{^{103}Rh} and ^{13}C-{^{31}P} measurements were carried out as described previously.[8,9] Carbon-13 chemical shifts are reported in p.p.m. from $SiMe_4$, ^{31}P chemical shifts in p.p.m. from external phosphoric acid, and, for $\delta(^{103}Rh)$, 0 p.p.m. = 3.16 MHz at such a magnetic field that the protons for $SiMe_4$ in $CDCl_3$ solution resonate at exactly 100 MHz; high-frequency shifts are positive.

Results

The solid-state structures of $[Rh_9E(CO)_{21}]^{2-}$ and $[Rh_{10}E(CO)_{22}]^{3-}$ are shown schematically in Figure 1. Each rhodium atom in both clusters is bonded to one terminal carbonyl, which has been omitted from the Figure for the sake of clarity.
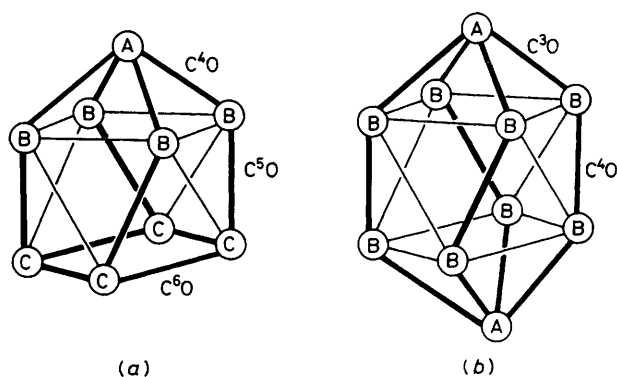

(a)   *(b)*

Figure 1. Schematic representation of (a) $[Rh_9E(CO)_{21}]^{2-}$ and (b) $[Rh_{10}E(CO)_{22}]^{3-}$ (E = P or As) showing the minimum reorganisation of the carbonyl skeleton which occurs on going from the Rh_9 to the Rh_{10} cluster. Each rhodium in both clusters has one terminal carbonyl group (Rh_A-C^1O, Rh_B-C^2O, Rh_C-C^3O) which has been omitted for clarity; bold lines indicate bridging CO groups

In $[Rh_9E(CO)_{21}]^{2-}$ there are three types of terminal carbonyls, Rh_A-C^1O, Rh_B-C^2O, and Rh_C-C^3O in the ratio 1 : 4 : 4, and for $[Rh_{10}E(CO)_{22}]^{3-}$ there are two types of terminal carbonyls, Rh_A-C^1O and Rh_B-C^2O in the ratio 2 : 8. The edge-bridging carbonyls in $[Rh_9E(CO)_{21}]^{2-}$ fall into three equally intense sets with C^4O bridging all Rh_A-Rh_B edges, C^5O bridging alternate Rh_B-Rh_C edges, and C^6O bridging all Rh_C-Rh_C edges. For $[Rh_{10}E(CO)_{22}]^{3-}$ there are two types of edge-bridging carbonyls, C^3O and C^4O in the ratio 8 : 4 with C^3O bridging all Rh_A-Rh_B edges and C^4O bridging alternate Rh_B-Rh_B edges.

Inspection of Figure 1 shows that there is minimal re-arrangement of the carbonyl polyhedron on going from the Rh_9 to the Rh_{10} cluster.

$[Rh_{10}E(CO)_{22}]^{3-}$ (E = P *or* As).— The low-temperature ($-91\ °C$) ^{13}C n.m.r. spectrum of $[Rh_{10}P(CO)_{22}]^{3-}$ in acetone is shown in Figure 2(c), together with the rhodium-decoupled [Figure 2(a) and (b)] and phosphorus-decoupled [Figure 2(d)] spectra, which allow unambiguous assignment. The undecoupled spectrum clearly shows four groups of resonances at 246.9, 238.8, 199.0, and 193.9 p.p.m. with relative intensities 4 : 8 : 2 : 8 due to C^4O, C^3O, C^1O, and C^2O respectively. All the resonances, except C^4O, show coupling to phosphorus,
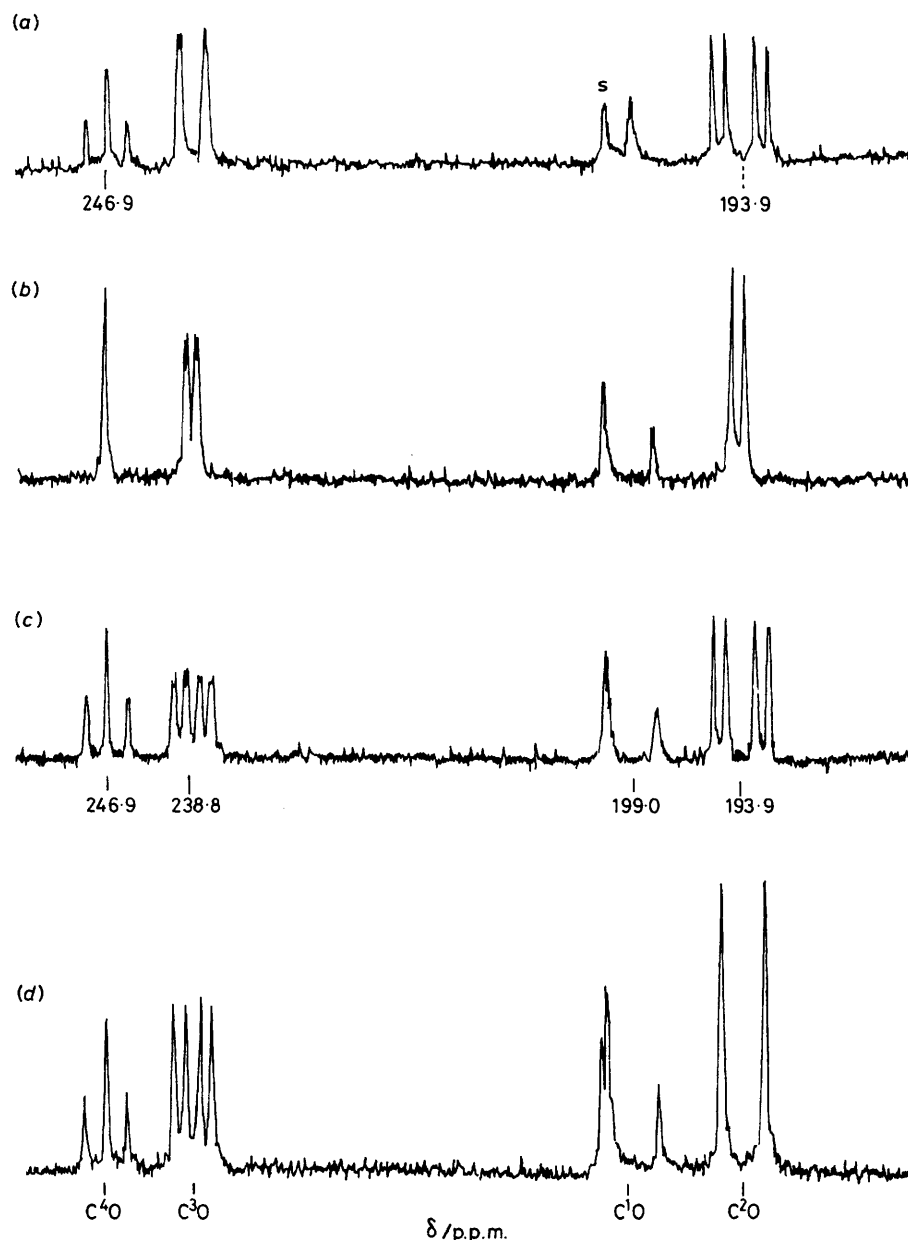
Figure 2. 25-MHz ^{13}C-{^{103}Rh} and ^{13}C-{^{31}P} n.m.r. spectra of [Cs{Me(OCH$_2$CH$_2$)$_4$OMe}]$_3$[Rh$_{10}$P(CO)$_{22}$] in (CD$_3$)$_2$CO at -91 °C: (a) decoupling Rh$_A$ [Ξ 3.158 097 MHz, δ(Rh$_A$) -607 p.p.m.]; (b) decoupling Rh$_B$ [Ξ 3.155 967 MHz, δ(Rh$_B$) -1 281 p.p.m.]; (c) undecoupled; (d) decoupling P [Ξ 40.496 150 MHz, δ(P) $+376.9$ p.p.m.]. S = solvent

which has been confirmed in the ^{13}C-{^{31}P} spectrum [Figure 2(d)]. ^{13}C-{^{103}Rh} Measurements show there to be two rhodium resonances (Ξ 3.158 097 and 3.155 967 MHz), which can be assigned to Rh$_A$ (-607 p.p.m.) and Rh$_B$ (-1 281 p.p.m.) respectively. Thus, decoupling Rh$_A$ [Figure 2(a)] causes the resonance due to C^{1}O at 199.0 p.p.m. to collapse and the resonance due to C^{3}O at 238.8 p.p.m. to become a doublet of doublets due to residual coupling to Rh$_B$ and to the interstitial phosphorus. Similarly, decoupling Rh$_B$ [Figure 2(b)] causes the resonance due to C^{4}O at 246.9 p.p.m. to become a singlet and the terminal carbonyl resonance due to C^{2}O at 193.9 p.p.m. collapses to a doublet due to residual interaction with the interstitial phosphorus. These data, together with those [10] for the corresponding clusters [Rh$_{10}$As(CO)$_{22}$]$^{3-}$ and [Rh$_{10}$S-(CO)$_{22}$]$^{2-}$ at low temperature, are summarised in Table 1. The

data for all three compounds are very similar with the different rhodium–carbon spin–spin coupling values to C^{3}O reflecting the different values of d(Rh$_A$–C^{3}O) 2.24 Å and d(Rh$_B$–C^{3}O) 1.92 Å caused through asymmetric bridging. When considering the wide range of ^{103}Rh chemical shifts that are presently known,[11] the variation for the compounds in Table 1 is not very large. It therefore seems probable that, in keeping with previous results,[12] the increased charge on going from the di- to the tri-anion is mainly dissipated onto the carbonyls as reflected by the mean carbonyl chemical shift moving to lower field with increased charge on the anion [δ(^{13}CO)$_{mean}$ = 215, 220.2, and 219.4 p.p.m. for E = S, P, and As respectively].

Variable-temperature ^{13}C n.m.r. spectra of [Rh$_{10}$P(CO)$_{22}$]$^{3-}$ show that all the carbonyl resonances broaden simultaneously

Table 1. N.m.r. data for $[Rh_{10}E(CO)_{22}]^{n-}$ (E = P or As, n = 3; E = S, n = 2) at low temperature

	E		
	P^{a}	As^{b}	S^{c}
$\delta(C^1O)$/p.p.m.	199.0	202.9	200.3
$\delta(C^2O)$/p.p.m.	193.9	194.6	192.5
$\delta(C^3O)$/p.p.m.	238.8	235.6	230.8
$\delta(C^4O)$/p.p.m.	246.9	244.8	236.9
$^1J(Rh_A-C^1O)$/Hz	103.5	115.7	109.9
$^1J(Rh_B-C^2O)$/Hz	90.3	93.6	94.6
$^1J(Rh_A-C^3O)$/Hz	25.4	26.1	27.5
$^1J(Rh_B-C^3O)$/Hz	53.7	55.6	55.0
$^1J(Rh_B-C^4O)$/Hz	43.9	43.2	42.7
$\delta(Rh_A)$/p.p.m.	−607	−495	$−755^{d}$
$\delta(Rh_B)$/p.p.m.	−1 281	−1 220	$−1 169^{d}$
$\delta(P)$/p.p.m.	$+376.9^{e}$		
$^2J(Rh_A-P)$/Hz	56^{e}		
$^1J(Rh_B-P)$/Hz	21^{e}		
$^2J(P-C^1O)$/Hz	5.9		
$^2J(P-C^2O)$/Hz	26.9		
$^2J(P-C^3O)$/Hz	5.9		

^{a} In $(CD_3)_2CO$. At −91 °C except where indicated. ^{b} In $(CD_3)_2CO$ at −95 °C. ^{c} In $[^2H_8]$tetrahydrofuran. At −82 °C except where indicated. ^{d} At −70 °C. ^{e} At −80 °C.

Table 2. N.m.r. data for $[Rh_9P(CO)_{21}]^{2-}$ in $[^2H_8]$tetrahydrofuran at low temperature (^{13}C and $^{13}C-\{^{103}Rh\}$ measurements at −99 °C, ^{31}P and $^{13}C-\{^{31}P\}$ measurements at −91 °C), together with the corresponding Rh−CO bond lengths (Å) in parentheses

$\delta(C^1O)$/p.p.m.	193.7	$\delta(Rh_A)$/p.p.m.	−1 413
$\delta(C^2O)$/p.p.m.	190.0	$\delta(Rh_B)$/p.p.m.	−1 243
$\delta(C^3O)$/p.p.m.	193.5	$\delta(Rh_C)$/p.p.m.	−1 049
$\delta(C^4O)$/p.p.m.	244.3	$\delta(P)$/p.p.m.	+282.3
$\delta(C^5O)$/p.p.m.	236.5		
$\delta(C^6O)$/p.p.m.	240.2	$^2J(Rh_A-P)$/Hz	34.0
$^1J(Rh_A-C^1O)$/Hz	97.3 (1.847)	$^1J(Rh_B-P)$/Hz	34.0
$^1J(Rh_B-C^2O)$/Hz	88.2 (1.852)	$^1J(Rh_C-P)$/Hz	46.0
$^1J(Rh_C-C^3O)$/Hz	95.6 (1.843)	$^2J(P-C^2O)$/Hz	30.3
$^1J(Rh_A-C^4O)$/Hz	24.3 (2.150)	$^2J(P-C^3O)$/Hz	31.7
$^1J(Rh_B-C^4O)$/Hz	52.8 (1.973)		
$^1J(Rh_B-C^5O)$/Hz	52.8 (1.934)		
$^1J(Rh_C-C^5O)$/Hz	22.5 (2.207)		
$^1J(Rh_C-C^6O)$/Hz	$\begin{cases} 49.1 \ (1.976) \\ 29.9 \ (2.150) \end{cases}$		

due to the onset of a concerted scrambling of *all* the carbonyl ligands rather than any localised fluxional process. In sulpholane (tetrahydrothiophene 1,1-dioxide) at +100 °C there is just one resonance at 221.3 p.p.m., which agrees well with the weighted average of the resonances in the spectrum in acetone solution at −90 °C (see above). However, this resonance is not a well resolved multiplet, as found for the corresponding $[Rh_{10}As(CO)_{22}]^{3-}$ (see below), but it is not possible to go to higher temperatures in order to produce the fast-exchange limiting spectrum.

A similar, but more facile, carbonyl fluxionality is observed for $[Rh_{10}As(CO)_{22}]^{3-}$. In this case, the resonances in both the 25- and 90.56-MHz low-temperature (−95 °C) spectra are significantly broader than those found for $[Rh_{10}P(CO)_{22}]^{3-}$ under the same conditions and, similarly, the fast-exchange carbonyl multiplet for $[Rh_{10}As(CO)_{22}]^{3-}$, observed at +91 °C in EtCN, is much better resolved than for $[Rh_{10}P(CO)_{22}]^{3-}$. The position of this multiplet [220.3 p.p.m., J(Rh−CO) 9.3 Hz] is again close to the mean value of the carbonyl chemical shifts in the low-temperature spectrum and the pattern and multiplicity suggests that polyhedral rearrangement of the metal skeleton is occurring. This has been confirmed by collapsing the multiplet to a single line with low-power irradiation at a single rhodium resonance frequency [Ξ 3.156 922 MHz, $\delta(Rh_{A,B})$ −972 p.p.m.], which is close to that expected from the value of $\delta(Rh)_{mean}$ −1 075 p.p.m. at −95 °C after allowing for solvent and temperature effects (*ca.* +0.6 p.p.m. per °C).

The same fluxional behaviour of both the carbonyl and metallic polyhedra also occurs in $[Rh_{10}P(CO)_{22}]^{3-}$. In this case, the behaviour of the metallic skeleton is best illustrated from variable-temperature ^{31}P n.m.r. measurements. At −80 °C in acetone solution the ^{31}P n.m.r. spectrum is clearly different from that observed at +76 °C in sulpholane solution. At −80 °C, the resonance $[\delta(^{31}P) +376.9$ p.p.m.] can be accurately simulated as a triplet, $^2J(Rh_A-P)$ 56 Hz, of nonets, $^1J(Rh_B-P)$ 21 Hz, whereas at +76 °C it is a well resolved undecet with $J(Rh_{A,B}-P) = 31.7$ Hz and $\delta(^{31}P) +366$ p.p.m. This clearly shows that the metallic skeleton is static at low temperature but becomes fluxional at high temperature. The time-averaged value of $J(Rh_{A,B}-P)$ at +76 °C is similar to the

weighted mean of $^2J(Rh_A-P)$ and $^1J(Rh_B-P)$ obtained at −80 °C. This suggests that both $^2J(Rh_A-P)$ and $^1J(Rh_B-P)$ at low temperature have the same sign, which is probably negative from previous studies.[13] It is also worth noting that $|^2J(Rh_A-P)| > |^1J(Rh_B-P)|$. This is rather surprising, but is similar to the data on J(Rh−Pt) found for $[PtRh_5(CO)_{15}]^{-}$,[14] and probably stems from the larger number of pathways available for transmission of spin–spin coupling in the two-bond case.

$[Rh_9E(CO)_{21}]^{2-}$ (E = P *or* As).—The variable-temperature ^{13}C n.m.r. spectra of $[Rh_9P(CO)_{21}]^{2-}$ are shown in Figure 3(a). At −90 °C, the spectrum is in accord with that expected from the solid-state structure and has been unambiguously assigned using a combination of $^{13}C-\{^{103}Rh\}$ and $^{13}C-\{^{31}P\}$ measurements, as described above for $[Rh_{10}P(CO)_{22}]^{3-}$. The resulting couplings are shown schematically in Figure 3(b) and the spectroscopic data are summarised in Table 2.

It should be noted that the resonance due to C^1O, which is coincident with C^3O in the 25-MHz spectrum, is clearly visible in the low-temperature 90.56-MHz spectrum and, whereas $^2J(P-CO)$ was observed for both terminal and edge-bridging carbonyls in $[Rh_{10}P(CO)_{22}]^{3-}$, there is only coupling of the terminal carbonyls, C^2O and C^3O, with the interstitial phosphorus in $[Rh_9P(CO)_{21}]^{2-}$.

As found for $[Rh_{10}P(CO)_{22}]^{3-}$, the edge-bridging carbonyls, C^4O, to the capping atom Rh_A in $[Rh_9P(CO)_{21}]^{2-}$ are approximately *trans* to each other; this leads to $d(Rh_A-C^4O) > d(Rh_B-C^4O)$, which is parallelled in the different values found for J(Rh−CO) (see Table 2). The other edge-bridging carbonyls, C^5O and C^6O, are also asymmetrically bridged because of a *trans*-$C^6O-Rh_C-C^5O$ configuration. This results in all Rh_C-Rh_B edges being asymmetrically bridged with an alternation of long and short Rh_C-C^6O bonds around the $[Rh_C]_4$ square face; similarly, $d(Rh_C-C^5O) > d(Rh_B-C^5O)$. This asymmetric bridging found in the solid state seems to be retained in solution as exemplified by the different values found for $^1J(Rh−CO)$ with short rhodium–carbonyl bonds giving rise to high values of $^1J(Rh−CO)$ (Table 2).

Variable-temperature ^{13}C n.m.r. measurements on $[Rh_9P(CO)_{21}]^{2-}$ show the simultaneous broadening of all the carbonyl resonances until a broad resonance is obtained at room temperature; this broad resonance collapses to a sharp doublet [J(P−CO) 12.2 Hz] on irradiation at a single rhodium resonance frequency [Ξ 3.156 347 MHz; $\delta(Rh)$ = −1 161 p.p.m.] which is close to $\delta(Rh)_{mean}$ −1 176 p.p.m. at −90 °C. This is in agreement with both the carbonyl and metal skele-

(a)

θc/°C

40
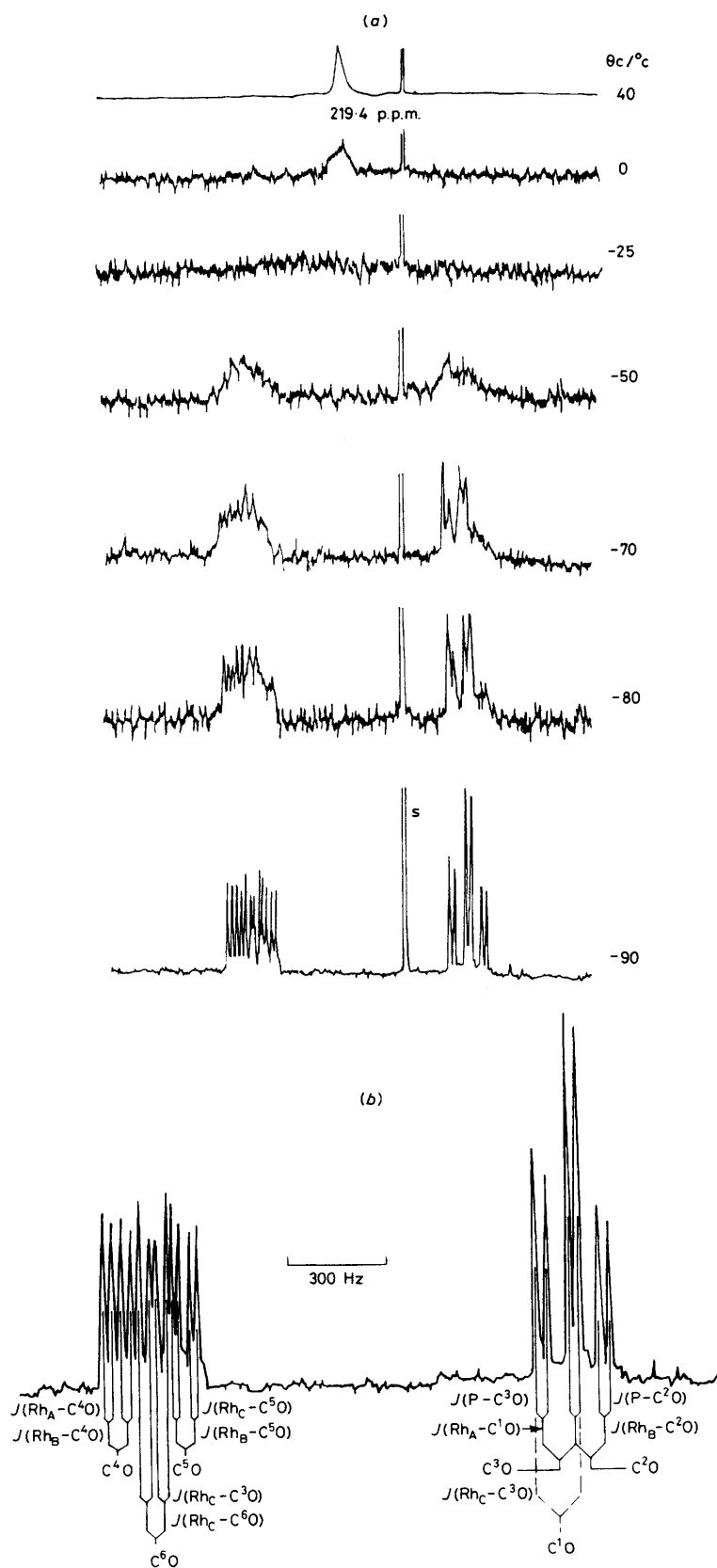
219·4 p.p.m.

0

-25

-50

-70

-80

s

-90

(b)

300 Hz

$J(Rh_A-C^4O)$

$J(Rh_B-C^4O)$

$J(Rh_C-C^5O)$

$J(Rh_B-C^5O)$

C^4O C^5O

$J(Rh_C-C^3O)$

$J(Rh_C-C^6O)$

C^6O

$J(P-C^3O)$

$J(Rh_A-C^1O)$→

C^3O

$J(Rh_C-C^3O)$

$J(P-C^2O)$

$J(Rh_B-C^2O)$

C^2O

C^1O

Figure 3. (a) Variable-temperature 25-MHz ^{13}C n.m.r. spectra of [Cs{Me(OCH$_2$CH$_2$)$_4$OMe}]$_2$[Rh$_9$P(CO)$_{21}$] in (CD$_3$)$_2$CO; (b) expansion of spectrum at −90 °C together with assignments (see Figure 1). S = solvent

(a)

(b)

Observed   Calculated

Figure 4. Observed and simulated ^{31}P n.m.r. spectra of [Cs{Me-(OCH$_2$CH$_2$)$_4$OMe}]$_2$[Rh$_9$P(CO)$_{21}$] in (CD$_3$)$_2$CO at (a) +25 °C [J(Rh$_A$-P) = J(Rh$_B$-P) = J(Rh$_C$-P) = 38.4 Hz] and (b) −80 °C [J(Rh$_A$-P) = J(Rh$_B$-P) = 34.0, J(Rh$_C$-P) = 46.0 Hz]

Figure 5. Schematic representation of the structure of [Rh$_{12}$Sb(CO)$_{27}$]$^{3-}$. Each rhodium is bonded to one terminal carbonyl, which has been omitted for the sake of clarity, and bridging carbonyls are indicated by the symbol ⧕

trum [Figure 4(a)] becomes a symmetrical decet due to equal couplings to all nine rhodium atoms [J(Rh$_{A,B,C}$-P) = 38.5 Hz] caused by randomisation of the rhodium polyhedron about the interstitial phosphorus. The time-averaged value of J(Rh$_{A,B,C}$-P) is close to the weighted mean of the low-temperature rhodium–phosphorus couplings and again implies that the rhodium–phosphorus spin–spin couplings observed at low temperature all have the same sign.

[Rh$_{12}$Sb(CO)$_{27}$]$^{3-}$.—The structure of this cluster, which is represented schematically in Figure 5, consists of a distorted icosahedral arrangement of rhodium atoms; each rhodium has one terminal carbonyl and the remaining 15 edge-bridging carbonyls are distributed as shown in the Figure.[5] It has not been possible to obtain the low-temperature limiting spectrum since the 90.56-MHz ^{13}C n.m.r. spectrum at −97.5 °C consists of only a broad resonance [δ(CO) 230.6 p.p.m.] due to the edge-bridging carbonyls and a broad doublet [δ(CO) 198.6 p.p.m., J(Rh-CO) 100.7 Hz] due to the terminal carbonyls. At room temperature, however, both the metallic and carbonyl skeletons become fluxional since 11 lines of the expected 13-line symmetrical multiplet are observed [δ(CO) 216.6 p.p.m., J(Rh-CO) 7.3 Hz] in the 25-MHz ^{13}C n.m.r. spectrum and low-power rhodium decoupling at a single frequency [Ξ 3.157 672 MHz, δ(Rh) −742 p.p.m.] collapses this multiplet to a singlet.

tons being fluxional, as suggested earlier from rhodium n.m.r. measurements,[4] and is further confirmed by variable-temperature ^{31}P n.m.r. measurements.

The low-temperature ^{31}P n.m.r. spectrum of [Rh$_9$P(CO)$_{21}$]$^{2-}$ is shown in Figure 4(b) and may be simulated as a triplet, ^2J(Rh$_A$-P) = 34 Hz, of quintets, ^1J(Rh$_B$-P) = 34 Hz, of quintets, ^1J(Rh$_C$-P) = 46 Hz. These values differ from those previously reported but reinspection of the rhodium spectrum shows that the apical rhodium–phosphorus coupling [^2J-(Rh$_A$-P) in Figure 2 of ref. 4] must be revised. It should also be noted that, because of our ^{13}C-{^{103}Rh} measurements, the direct ^{103}Rh n.m.r. assignments of the rhodium resonances previously attributed to the two sets of inequivalent square-antiprismatic rhodium atoms, Rh$_B$ and Rh$_C$ (Figure 1),[4] must now be reversed. At room temperature, the ^{31}P n.m.r. spec-
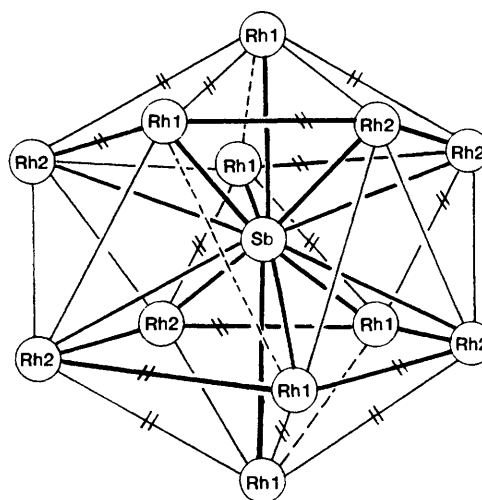
Discussion

Comparison of the variable-temperature ^{13}C n.m.r. spectra of [Rh$_9$E(CO)$_{21}$]$^{2-}$ and [Rh$_{10}$E(CO)$_{22}$]$^{3-}$ shows that, in both cases, carbonyl fluxionality is more facile when E = As than when E = P. As both carbonyl and metal polyhedral rearrangements in the above compounds appear to be interconnected, it seems probable that this stems from an expansion of the metal skeleton which is necessary in order to accommodate the larger interstitial arsenic atom {for [Rh$_{10}$E-(CO)$_{22}$]$^{3-}$ d(Rh$_A$-Rh$_B$) = 2.841 and 2.869 Å and d(Rh$_B$-Rh$_B$) = 2.859 and 2.895 Å for E = P and As respectively}. This would be expected to result in a lower activation energy for randomisation of metal atoms in the less strongly bound arsenido-species and this would, in turn, lower the activation energy for carbonyl migration.
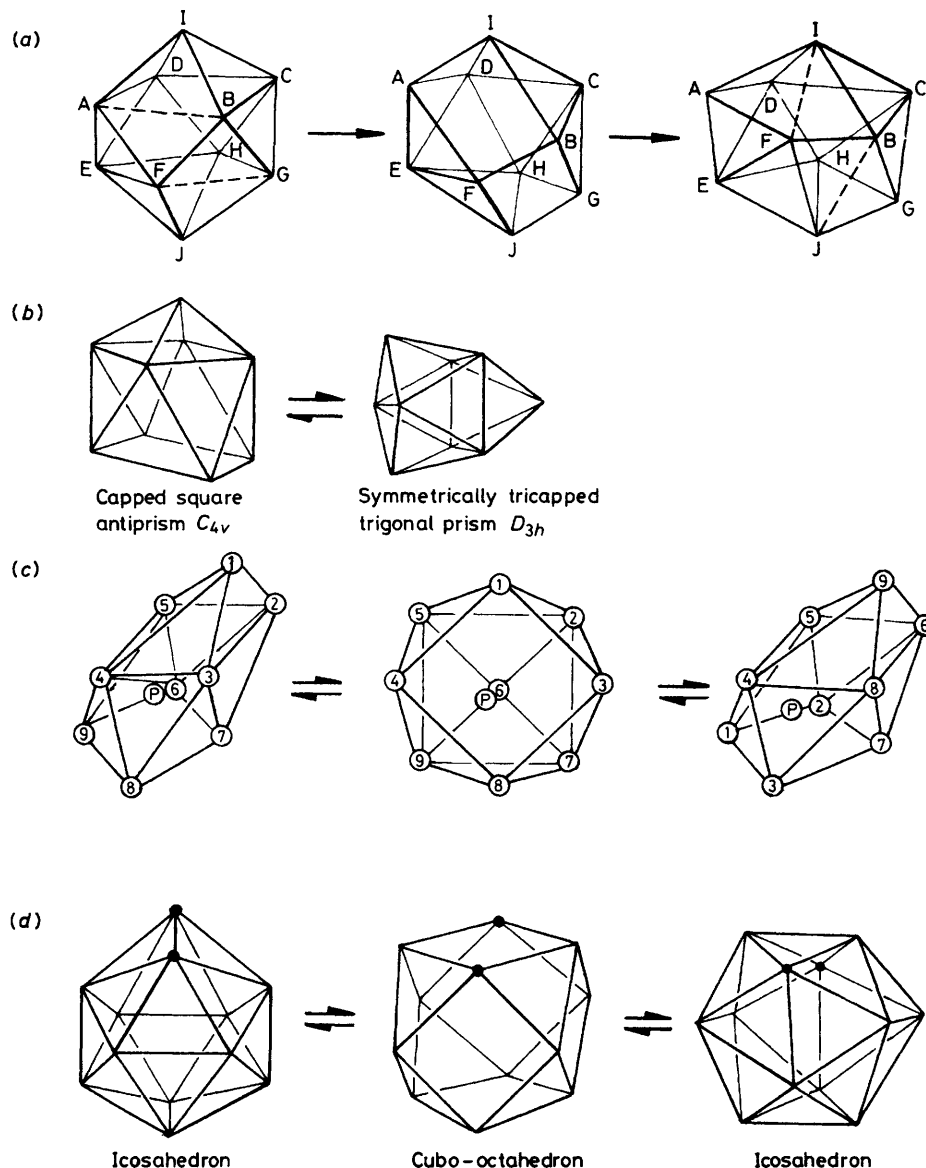
Figure 6. Schematic representation of the possible mechanisms for metal skeletal rearrangements of (a) $[Rh_{10}E(CO)_{22}]^{3-}$, (b), (c) $[Rh_9E(CO)_{21}]^{2-}$, and (d) $[Rh_{12}Sb(CO)_{27}]^{3-}$

Although it is impossible to define exactly the migratory pathways of the metallic skeletons, it seems probable that they are related to similar rearrangements found for boron polyhedra in boron hydrides. Thus, the fluxionality of the boron cage in $[B_{10}H_{10}]^{2-}$ has been proposed [15] to occur by the concerted process shown in Figure 6(a) and a similar rearrangement could be involved in the Rh_{10} clusters. Similarly, rearrangement of the C_{4v} Rh_9 capped-square-antiprismatic skeleton via a D_{3h} tricapped trigonal prism [Figure 6(b)] as proposed for boranes and other nine-atom clusters [16,17] could account for randomisation of the Rh_9 polyhedron, although it is also feasible that a concerted rhodium–rhodium bond-breaking and -making process [Figure 6(c)] could be involved.

For $[Rh_{12}Sb(CO)_{27}]^{3-}$ the presence of three long rhodium–rhodium bonds probably facilitates metal polyhedral rearrangement, which is perhaps similar to that reported for 1,2-dicarba-closo-dodecaborane, $1,2-C_2B_{10}H_{12}$ [Figure 6(d)],[18] as previously suggested on the basis of the solid-state structure.[5]

Finally, it should be noted that for rhodium carbonyl clusters containing interstitial metal atoms, $[Rh_{13}(CO)_{24}-H_{5-n}]^{n-}$ ($n = 1$—4) [19] and $[Rh_{14}(CO)_{24}H_{4-n}]^{n-}$ ($n = 3$ or 4),[12] we have no evidence for rearrangement of the metallic skeleton. In these cases, there is probably a more compact rigid metallic skeleton than is possible for clusters containing interstitial heteroatoms.

Acknowledgements

References

1 J. L. Vidal, W. E. Walker, R. L. Pruett, and R. C. Schoening, Inorg. Chem., 1979, 18, 129.
2 J. L. Vidal, Inorg. Chem., 1981, 20, 241.

3 J. L. Vidal, W. E. Walker, and R. C. Schoening, *Inorg. Chem.*, 1981, **20**, 238.

4 O. A. Gansow, D. S. Gill, F. J. Bennis, J. R. Hutchinson, J. L. Vidal, and R. C. Schoening, *J. Am. Chem. Soc.*, 1980, **102**, 2449.

5 J. L. Vidal and J. H. Troup, *J. Organomet. Chem.*, 1982, **213**, 351.

6 J. L. Vidal, W. E. Walker, R. L. Pruett, and R. C. Schoening, *Inorg. Chem.*, 1979, **18**, 1821.

7 B. T. Heaton, L. Strona, S. Martinengo, D. Strumolo, R. J. Goodfellow, and I. H. Sadler, *J. Chem. Soc., Dalton Trans.*, 1982, 1499.

8 C. Brown, B. T. Heaton, L. Longhetti, W. T. Povey, and D. O. Smith, *J. Organomet. Chem.*, 1980, **192**, 93.

9 B. T. Heaton, L. Longhetti, L. Garlaschelli, and U. Sartorelli, *J. Organomet. Chem.*, 1980, **192**, 431.

10 L. Garlaschelli, A. Fumagalli, S. Martinengo, B. T. Heaton, D. O. Smith, and L. Strona, *J. Chem. Soc., Dalton Trans.*, 1982, 2265.

11 R. G. Kidd and R. J. Goodfellow, in ' N.M.R. and the Periodic Table,' eds. R. K. Harris and B. E. Mann, Academic Press, London, 1978, 244.

12 B. T. Heaton, C. Brown, D. O. Smith, L. Strona, R. J. Goodfellow, P. Chini, and S. Martinengo, *J. Am. Chem. Soc.*, 1980, **102**, 6175.

13 E. M. Hyde, J. D. Kennedy, B. L. Shaw, and W. McFarlane, *J. Chem. Soc., Dalton Trans.*, 1977, 1571.

14 A. Fumagalli, S. Martinengo, P. Chini, A. Albinati, S. Bruckner, and B. T. Heaton, *J. Chem. Soc., Chem. Commun.*, 1978, 195.

15 E. L. Muetterties, ' Boron Hydride Chemistry,' Academic Press, New York, 1975.

16 L. J. Guggenburger and E. L. Muetterties, *J. Am. Chem. Soc.*, 1976, **98**, 7221.

17 R. W. Rudolph, W. L. Wilson, F. Parker, R. C. Taylor, and D. C. Young, *J. Am. Chem. Soc.*, 1978, **100**, 4629.

18 W. N. Lipscomb, *Science*, 1966, **153**, 373.

19 S. Martinengo, B. T. Heaton, R. J. Goodfellow, and P. Chini, *J. Chem. Soc., Chem. Commun.*, 1977, 39.